Effects of surface roughness on quasi-one-dimensional and -two-dimensional ballistic channels

Mizuho K. Schwalm* and William A. Schwalm*
Department of Physics, Montana State University, Bozeman, Montana 59717
(Received 23 April 1991; revised manuscript received 21 November 1991)

Effects of rough boundaries on electron transport in tight-binding, quasi-one-dimensional (Q1D) and quasi-2D (Q2D) channels are studied. The Q1D channels have uncorrelated edge roughness over a distance that is long compared with the width, and are connected to semi-infinite, perfect leads. The Q2D channels have uncorrelated washboardlike edge roughness with translation symmetry perpendicular to the current flow. The standard Green-function method is applied with high resolution to the Q1D sample while the leads are treated exactly by a Green-function extension theory [Phys. Rev. B **37**, 9524 (1988)]. The extension theory also gives the density of states and Kubo-Greenwood conductance of the Q2D case exactly in terms of Q1D results. Analytical results are presented for the conductance of ordered cases. In the Q1D case, it is found that edge roughness can create gaps in the spectrum and induce strongly localized states, similar to states found in quantum percolation. No such gaps or isolated states appear in the Q2D case. However, localized states with energies in the band continuum, but decoupled from the current-carrying states, cause a reduction in conductance for Fermi energy in a certain range. For comparison several Q1D models with periodic edge roughness are also studied.

Recent progress in the fabrication of quantum wells and quantum wires has stimulated theoretical work on the effects of geometry on ballistic electron transport. The model calculations presented here are to assess the effects of elastic scattering from boundary roughness on conductance of quasi-one-dimensional (Q1D) quantum wires or quasi-2D (Q2D) quantum wells. The focus of the paper is on the effects of surface roughness, which are interference effects controlled by geometry, on zero-field, zero-temperature, dc conductance. We treat both the Q1D case and a limited version of the Q2D case in which the electron is confined to a layer of limited thickness but which is of infinite extent in 2D.

A treatment of wave interference effects due to rough interface scattering developed by Tešanović, Jarić, and Maekawa[1] has been used by several authors.[2–4] In that method surface roughness is transformed into a pseudopotential perturbation of the smooth-surface problem. The strength of the pseudopotential is governed by $\lambda=\ln[a/a(\mathbf{x}_\parallel)]$, where a is the unperturbed width of the conducting channel and $a(\mathbf{x}_\parallel)$ is the actual width which fluctuates as a function of the position $\mathbf{x}_\parallel$ parallel to the surface. Under certain simplifying assumptions[1] the conductivity can be computed from the Kubo-Greenwood formula in terms of the correlation $\langle w(\mathbf{q})w(-\mathbf{q})\rangle$, where $w(\mathbf{q})$ is the Fourier transform of $\lambda(\mathbf{x}_\parallel)$. This calculation involves a further assumption in neglecting higher-order correlations in surface roughness.[4,5]

Different approximations are made in the work presented here in which a standard nearest-neighbor tight-binding Hamiltonian[6–8] is used to represent surface roughness. Model geometries are defined in Fig. 1. One can think of the Hamiltonian as a discrete approximation to the Schrödinger equation which should agree with the wave mechanical treatment in the effective mass or long-wavelength limit. Alternatively, discreteness of the model can represent true atomic granularity, which is important for narrow channels. Within this model the problem of a Q1D strip with rough edges is solved exactly by the method of Lee and Fisher.[9] The ordered, semi-infinite leads are treated exactly by a Green-function extension theory.[10] In the Q2D case, one further model approximation is introduced. The surface roughness is assumed

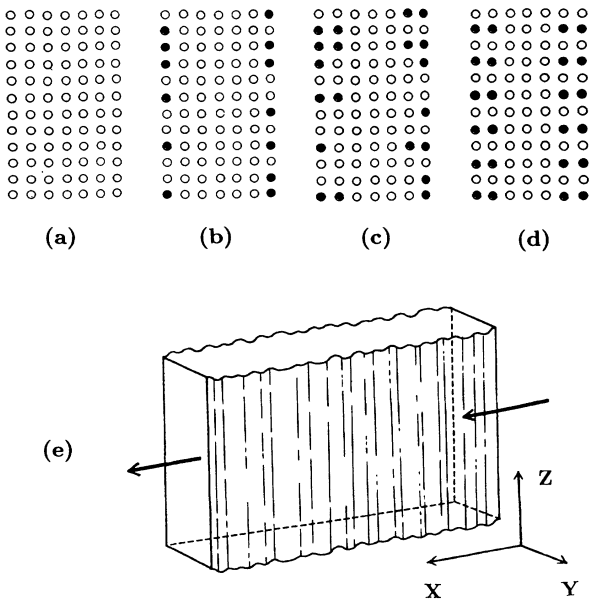

FIG. 1. Model geometries. (a)–(d) show diagonal elements of the tight-binding Hamiltonian in real space. Circles represent vertices in real space. Filled circles indicate missing atoms. The random surface roughness is increased from left to right in (a)–(c). (d) Ordered rough edge. (e) A schematic diagram of the washboardlike model. Conductances are measured in the x direction. The sample is extended to infinity in both the x and z directions. The width in the y direction is about 10 layers.

to have washboardlike translation symmetry along the surface in the direction perpendicular to the current flow as shown in Fig. 1(e). Thus the problem separates, and results can be obtained via the extension theory. No perturbation expansion is made in the amplitude of surface roughness and all orders of roughness correlation are taken fully into account within the linear-response theory. The current work is not primarily concerned with the length scaling of conductance, but rather with the effects on its energy variation due to surface conditions.

In the slice-recursion method of Lee and Fisher, Q1D samples are divided into slices consisting of rows of atoms. A Q1D sample region is connected to semi-infinite Q1D leads, and then Green functions $G=[z-H]^{-1}$ are calculated recursively, one slice at a time, through $G=g+gVG$, where g contains the matrix of Green functions for the region including up to the previous slice and also the disconnected slice. V represents the connection between the slice and the completed region. The roughness disorder is embedded in the Hamiltonian matrix H_n for the nth slice. In all models treated below, the sample region is 80 atoms long and the leads are infinite. The width of Q1D strips is 10 atoms.

To begin the slice-recursion process, Green functions for the lead regions at each end are computed exactly. This is possible because the Hamiltonian separates into additive x and y components, thus the eigenfunctions factor into x- and y-dependent parts. Owing to this separation of variables, the Green functions are expressed as convolutions involving Green functions for the x and y directions separately. If Green functions are known for two Hamiltonians H and K, defined on lattices $\mathcal{V}(H)$ and $\mathcal{V}(K)$, the extension theory in Ref. 10 gives Green functions for any Hamiltonian H_e in the product algebra of H and K through convolution integrals. Likewise, in certain circumstances conductance of blocks or of whole devices can also be obtained by convolution from conductance of lower-dimensional parts. Use is made below of this convolution formula to obtain conductance of the Q2D model of Fig. 1(e) from the Q1D results. A similar formalism giving conductance via convolutions has been developed by Bagwell[11] using continuous wave functions rather than discrete, tight-binding representation. The two formalisms must agree in the long-wavelength limit.

Analytical forms of Q1D-strip Green functions or conductance for ordered parts are obtained straightforwardly. These ordered cases therefore give both a convenient reference for which exact results are known and starting points from which the current response of the lead regions is obtained.

For the study reported here, the zero-field dc conductance is found via the Kubo-Greenwood formula, Eq. (3) in Ref. 9. The relation between the Kubo-Greenwood formula and the Landauer-type approach[12] using transmission matrices for the two-probe, 1D case[13] and for higher dimensions[14] and multiple-channel cases [15] has been investigated by other authors.

In the case of perfect order there are several exact results to which one can compare. In a 1D chain with diagonal energies 0 and off-diagonal energies $+1$, the band extends from -2 to $+2$. Since the density of states (DOS) exactly cancels the group velocity, it is well known that the conductance is proportional to[12]

$$\Gamma_1(E)=\Theta(4-E^2)\ , \tag{1}$$

where $\Theta(E)$ is the Heaviside step function. The multichannel conductance in a strip N sites wide can be found, for example, by the methods of Ref. 10, namely

$$\Gamma(E)=\int \Gamma_1(x)D(E-x)dx\ , \tag{2}$$

where $D(E)$ is the total density of states of a chain of length N, or

$$D(E)=\sum_{n=1}^{N}\delta(E-2\cos[n\pi/(N+1)])\ , \tag{3}$$

thus

$$\Gamma(E)=\sum_{n=1}^{N}\Theta(4-\{E-2\cos[n\pi/(N+1)]\}^2)\ . \tag{4}$$

One can understand the result Eq. (4) [and in fact the general formula Eq. (2)] in terms of the general result[12] that Γ, which is conductance in units of e^2/h, equals the number of channels or transverse modes available at Fermi energy E.

As the width $N\to\infty$, the conductance diverges proportionally. Thus one must readjust the normalization by using the 1D DOS *per site*,

$$D(E)=\frac{1}{\pi}(4-E^2)^{-1/2}\Theta(4-E^2)\ , \tag{5}$$

in Eq. (2). The resulting conductance for a perfect sheet is

$$\Gamma(E)=\left[\frac{1}{2}+\frac{1}{\pi}\sin^{-1}\left[\frac{2-|E|}{2}\right]\right]\Theta(16-E^2)\ . \tag{6}$$

Thus the conductance in a perfect tight-binding model of a 2D sheet, though it diverges as a function of sheet width, has this characteristic dependence on Fermi energy E. Equations (4) and (6) are plotted in Figs. 2(a) and 2(b). The conductance obtained by He and Das Sarma[6] using essentially the same numerical method as that used below in this work also shows the shape defined by Eq. (4) for the empty channel conductance as shown in Fig. 2(a).

The conductance spectra in Fig. 2 are symmetric with respect to $E=0$ reflecting the bipartite symmetry of the lattice Hamiltonian.[16] The number of steps on each side of the conductance curve in Fig. 2(a) is the same as the number of sites in the transverse direction. The quantized conductance steps have been a popular topic since first discovered.[17,18] A variety of different methods and models have been used to compute ballistic transport properties.[19–27] Regardless of the diversity of method, these calculations are able to predict conductance steps as a function of Fermi energy, wave number, or the width of a channel constriction.

One can stack sheets together to find the functional form of conductance along a perfect Q2D channel of infinite length and width and having a thickness of N sites. Thus $\Gamma_1(E)$ in Eq. (2) is supplied by the sheet result

$\Gamma(E)$ in Eq. (6) and $D(E)$ for a chain of N sites is supplied by Eq. (3). The result for a channel of width N is

$$\Gamma(E)=\sum_{n=1}^{N}\left[\frac{1}{2}+\frac{1}{\pi}\sin^{-1}\left[\frac{2-|E-E_n|}{2}\right]\right]\times\Theta(16-(E-E_n)^2)\ , \tag{7}$$

where

$$E_n=2\cos\left[\frac{n\pi}{N+1}\right]\ .$$

Again the limiting case $N\to\infty$ requires readjusting the normalization. One can use the 1D chain conductance Eq. (1) and the 2D DOS per site

$$D(E)=\frac{4}{\pi^2(4+|E|)}K\left[\frac{4-|E|}{4+|E|}\right]\Theta(16-E^2)\ , \tag{8}$$

where K is the complete elliptic integral of the first kind, or else one can use the 2D conductance Eq. (6) and the 1D DOS per site from Eq. (5). The conductance curve for $\Gamma(E)$ given by Eq. (7) is shown in Fig. 2(c).

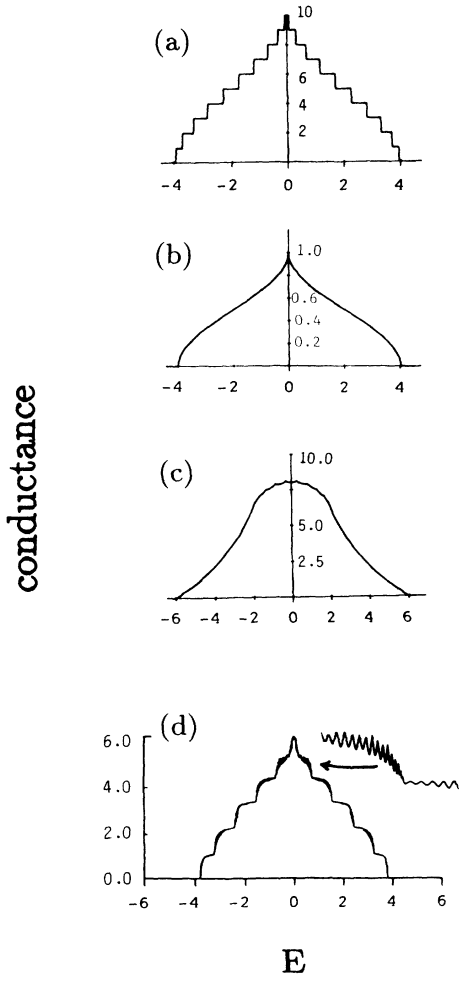

FIG. 2. Q1D conductance in ordered models. The Fermi energy E is measured in terms of the off-diagonal H matrix element. Units of conductance Γ are e^2/h. (a)–(c) Analytical results, Eqs. (4), (6), and (7), for dc conductance as a function of Fermi energy E. (a) Q1D with a finite width $N=10$. The value of Γ at $E=0$ is N. (b) perfect sheet. The height is normalized to 1. (c) Q2D sheet with 3D thickness $N=10$. (d) Numerical dc conductance for a Q1D strip with constriction. Length is $L=80$ and constriction width $N_b=6$ in channel of width $N_a=10$.

When conductance is computed from tight-binding Green functions, as it is for the rough channel treated in this work, the damping parameter η must be handled carefully. It should be noted that if a transmission formalism were used in which wave amplitudes are computed rather than Green functions, then no such damping would be necessary since the system is infinite. Spectral properties are derived from Green functions by adding a small imaginary part to make the energy variable $z=E+i\eta$ complex. The computation becomes singular in the limit $\eta\to 0$ which is of physical interest. So a small finite η is retained. For all data shown in this paper the resolution is fixed by dividing the entire spectrum into 8192 points, and η is set to the same as the step size. Thus the resolution should in all cases be less than the width of the lines used in drawing the curves.

Roughness is introduced by making the diagonal energies on certain randomly chosen edge sites very large compared to the off-diagonal elements as illustrated by the black dots in Fig. 1. This is equivalent to removing sites at random. The random perturbation is uncorrelated along the channel direction. If second-layer roughness is included, the second-layer sites adjacent to edge sites may also be void as determined by a conditional probability, given that the adjacent first-layer site is void.

Numerical dc conductance $\Gamma(E)$ for a Q1D strip with constriction is shown in Fig. 2(d) where the two outer rows of sites on each side of the 81 column sample region are essentially removed by making diagonal elements very large, hence the sample region is narrower than the leads. The overall shape of the conductance curve resembles the ordered Q1D strip case in Fig. 2(a) except that the number of steps is reduced to six, which is the number of rows of remaining sites. The sharp conductance steps are rounded somewhat and rapid oscillations are introduced, as has been discussed by several authors.[19,27] The physical origin of the rapid oscillations is well understood. This structure in $\Gamma(E)$ is due to an open-pipe standing-wave condition in which the length of the constricted channel, corrected for end effects, is an integer number of electron half wavelengths at the Fermi energy.[19]

Charge-density contours inside the Q1D strip in Figs. 3(a)–3(c) are computed by integrating the local densities of states (LDOS) projected on each site over the energy range $-4<E<-3$ from perfect channel in Fig. 3(a) to moderate roughness. One sees a region of charge depletion where electrons are repelled as the disorder increases. Features in the charge density in Figs. 3(a) and 3(b) correspond to individual voids. Level contours for LDOS at $E=0$ at each site are shown in Figs. 3(d) and 3(e). Figure 3(d) shows a standing-wave localized state at $E=0$ induced by a single missing atom at the edge where the arrow in the figure indicates the position of the miss-

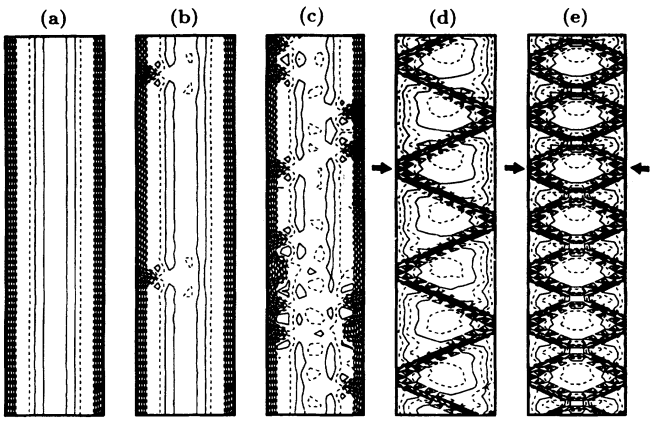

FIG. 3. Level contours of charge density presented for several values of surface roughness. (a)–(c) LDOS is integrated between -4 and -3. As random surface roughness increases, charge is forced away from the vacancies. (d) Electron is scattered at a single void indicated by the arrow. (e) Another void is introduced at the opposite side of the sample.

ing atom. The amplitude continues to reflect from edge to edge along the channel. The combined effect of two vacant sites on opposite sides is shown in Fig. 3(e). The precise nature of such $E=0$ states, which also occur in quantum percolation studies on a square lattice, is discussed below.

Figure 4 shows the total densities of states and dc conductance of a Q1D strip as a function of Fermi energy and surface roughness. p is the probability that a void occurs at a given site at an edge. The roughness reaches a maximum when $p=0.5$ since this is between the smooth channel and the constriction case. $p=0.5$ on the edge sites and also there is a conditional probability of 0.5 on the second layer in Fig. 4(c) where localized states appear to result at $E=0$. The sharp peak in the average DOS per site corresponds to zero conductance at $E=0$, and a gap opens in the conductance around $E=0$ as the number of rough layers increases to two. The average DOS per site in the central portion of the sample is computed at fixed energy by summing the local DOS at each active site within the central 81 slices of the sample region and then dividing by the number of active sites. Thus the area under each DOS curve in Fig. 4 is normal-

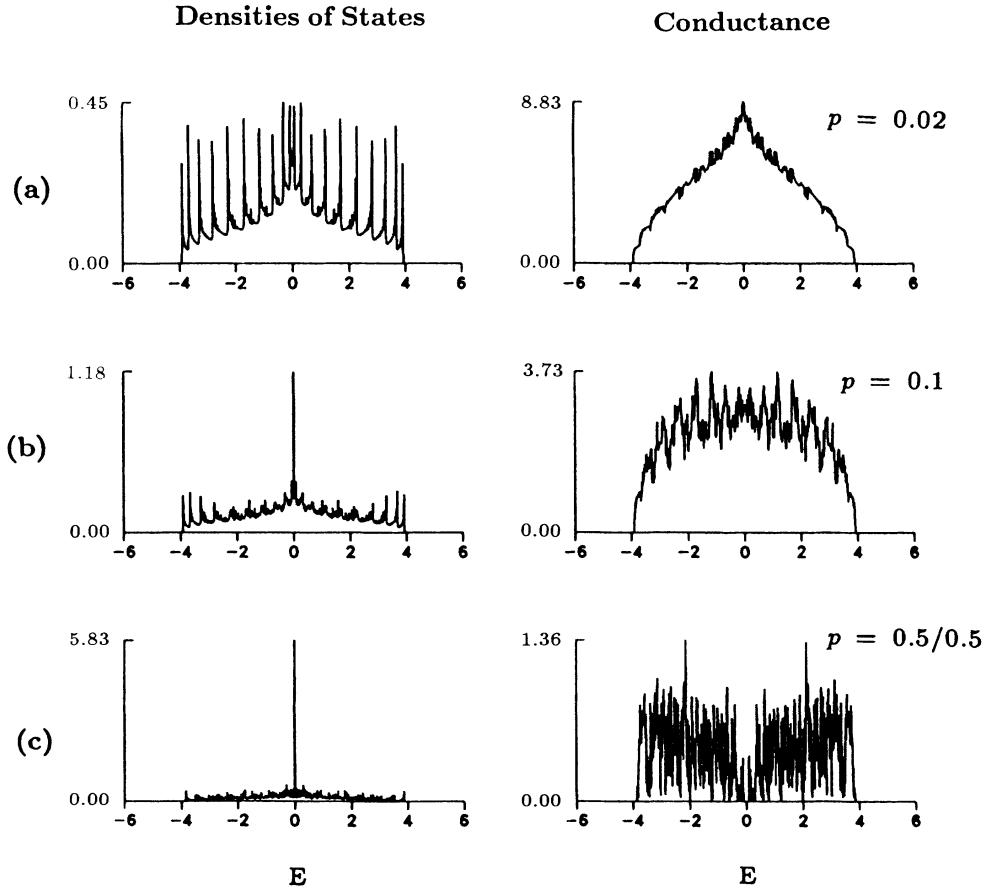

FIG. 4. Density of states and dc conductance of a Q1D strip as a function of Fermi energy and surface roughness. The units of Fermi energy E are the off-diagonal H matrix element V. Units of conductance Γ are e^2/h. (a) $p=0.02$, (b) $p=0.1$, and (c) $p=0.5$ with second-layer conditional probability 0.5.

ized to 1. The area under the $E=0$ peak is 0.5% in Fig. 4(b) and 2.0% in Fig. 4(c). The peaks are reproducible using different random roughness configurations. Note also that the effects of edge roughness are much more pronounced near the center of the band as opposed to the band edges. We shall return to this point.

In order to compare against the standard perturbation technique, we computed Green functions within the average propagator approximation.[5] For simplicity, we took the case of maximum disorder ($p=0.5$) with roughness involving only the outermost rows. For a finite barrier potential β, the perturbation on each edge site is divided into a constant $\frac{1}{2}\beta$ and a randomly fluctuating part with zero mean value. When the Born expansion for the Green functions is averaged over disorder, the noncanceling terms each contain only successive scatterings from the same edge site for some collection of edge sites. Since the distribution of site potentials is not Gaussian, it is a further approximation that we have also dropped higher than second cumulants from the averaged series expansion.[5] Finally, we performed a Dyson summation over all scattering events with self-energy consisting of diagrams with two successive scatterings from one site on the top layer or one site on the bottom layer. The infinite summation thus consists of all combinations of any number of such top- and bottom-layer scattering pairs. Except for the transformation to a pseudopotential, this calculation is in a spirit very similar to that of the method of Ref. 1. The resulting Green functions are well behaved as $\beta\rightarrow\infty$. The DOS computed this way is a smooth curve showing neither the gap nor the peak on the DOS at $E=0$. That no isolated $E=0$ peak results should not be surprising, since to include the effect of localized states requires including diagrams with any arbitrary number of coherent scatterings from the same site, which we have not done. If one wants to obtain evidence of well-localized states, then averaging over edge configurations is probably not the right thing to do.[28] It is less clear why the average propagator does not reproduce the gap around $E=0$.

Since gaps in the spectrum could be induced by periodic edge perturbations representing Fourier components of the spatial variation of random roughness, it is interesting to consider the case of ordered periodic edges. We have computed the band structure of several Q1D channels with periodic rough edges. In each case, the width alternates from a maximum N_a to a minimum N_b so that the period of variation is two atomic distances [see Fig. 1(d)]. Corresponding to edge roughness involving one or two outer layers we have chosen $N_b=N_a-2$ or $N_b=N_a-4$, preserving reflection symmetry of the channel.

First consider the case $N_a=5$ with $N_b=3$. There are five bands with even reflection symmetry, including one with $E=0$, and three with odd, including another $E=0$ band [Fig. 5(a)]. The dispersion formulas for the $E\neq0$ even bands are

$$E(k)=\pm\left[(5/2)+4c^2\pm\frac{(1+128c^2)^{1/2}}{2}\right]^{1/2}, \tag{9}$$

where $c=\cos(k)$ with k the wave number (atomic spacing $=1$). For the $E\neq0$ odd bands,

$$E(k)=\pm(1+4c^2)^{1/2}. \tag{10}$$

Thus, the overall bandwidth is $w=2[(13+\sqrt{129})/2]^{1/2}=6.980$ and there is a direct gap of width $\Delta_0=\frac{1}{2}(15/2)^{1/2}=1.369$ containing the $E=0$ states. The latter have zero mobility and do not contribute to the conductance. Wave amplitudes on the sites at the edge decrease rapidly for E close to the band extremes.

The $E=0$ states always appear when N_a is odd and $N_b=N_a-2$. The general pattern of wave amplitudes is illustrated by the case $N_a=7, N_b=5$ depicted at $k=0$ in Fig. 6. The even $E=0$ state in such models bare close relation to the localized states in the random model which give the $E=0$ peak.

In an infinite 2D square lattice, there are $E=0$ solutions to the tight-binding Schrödinger equation, each consisting of a diagonal chain of sites with wave ampli-

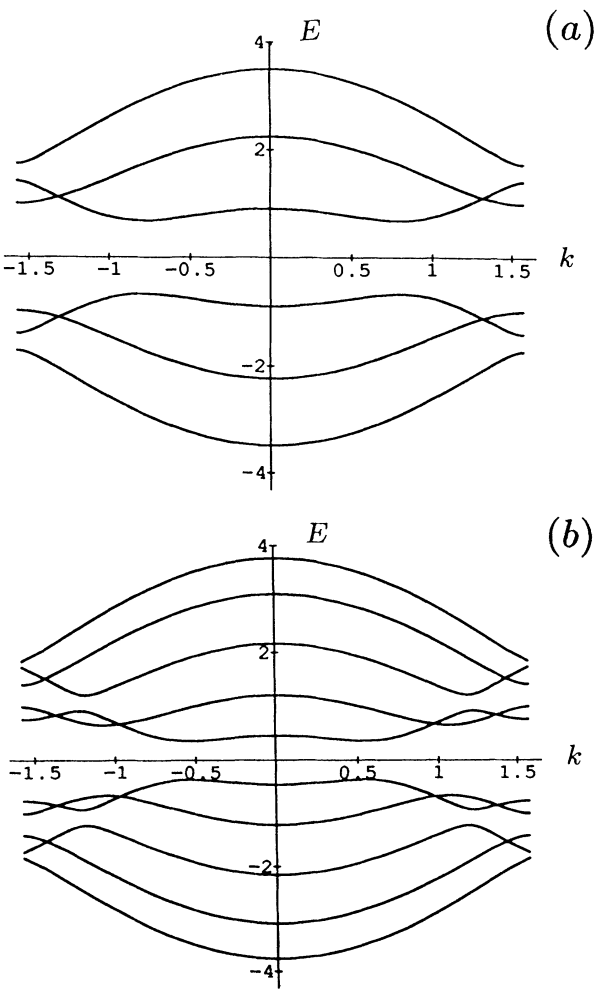

FIG. 5. Energy band for Q1D ordered rough edge. (a) Maximum width $N_a=5$ and minimum width $N_b=3$. (b) $N_a=7$, $N_b=5$. There are N_a even states and N_b odd states. Both models have one even and one odd $E=0$ solution. These flat $E=0$ bands are not shown.

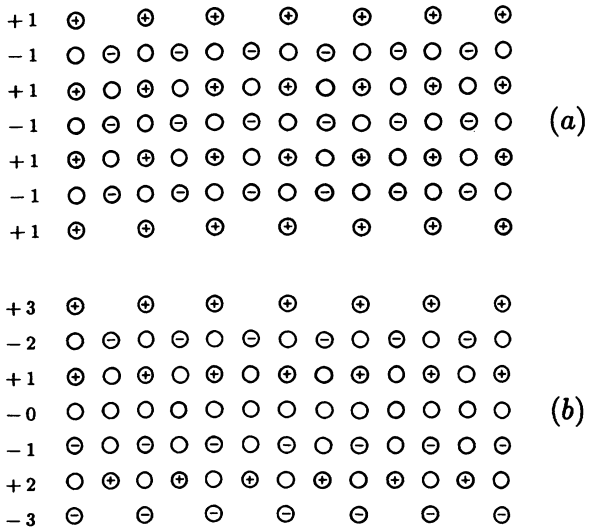

FIG. 6. Wave amplitudes for $E=0$ states of an ordered Q1D model with $N_a=7, N_b=5$ at $k=0$. (a) Even state, (b) odd state. Numbers at the left column are the amplitudes.

tudes alternating between $+1$ and -1. Since all such chain states are degenerate, they can be chosen in any combination. When there are missing sites or finite boundaries, an alternating chain state can terminate at a site with only two neighbors. At an edge, chain state can reflect. The reflection and termination are illustrated in Fig. 7. This phenomenon explains the charge-density contours shown for $E=0$ in Figs. 3(d) and 3(e).

The even $E=0$ states shown in Fig. 6(a) can be visualized as consisting of an array of chain states. When disorder is introduced in the edge roughness, a chain state can still exist, provided that it originates at a state with two neighbors, reflects zero or more times, and terminates at another two-neighbor site. These states are strictly localized. Though such states are geometrically forbidden in the ordered models with N_a even or $N_b \neq N_a - 2$, they can be induced by disorder.

As N_a becomes larger while remaining within the family $N_b = N_a - 2$ with N_a odd, the gap about $E=0$ becomes narrower and other gaps are formed. For example, when $N_a=7, N_b=5$, the width of the spectrum is $w=7.512$

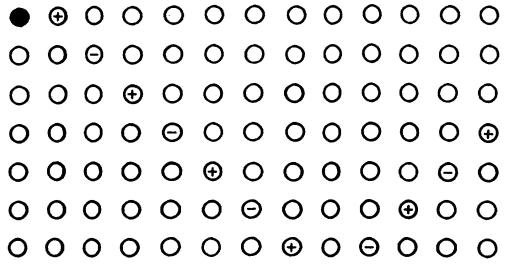

FIG. 7. Amplitude pattern for the diagonal chain state with $E=0$, showing termination and reflection. The black dot is a missing atom. Reflection can be thought of as a combination of two chains canceling so as to satisfy edge boundary condition.

while the central gap (which is always direct) has width $\Delta_0=0.731$. There is also a new, very narrow, indirect gap extending from $E=[(11-\sqrt{65})/2]^{1/2}=1.212$ at $k=0$ to $E=1.220$ at finite k. The width is thus $\Delta_1=0.008$, which is small but nonzero. The bipartite symmetry $E \rightarrow -E$ locates a corresponding gap in the lower half of the spectrum.

The bands for cases $N_a=5, N_b=3$ and $N_a=7, N_b=5$ described above are shown in Fig. 5. For contrast, it is interesting to consider cases not in the sequence $N_b=N_a-2$ for odd N_a.

For the $N_a=6, N_b=4$ case, $w=7.317$. As expected, there are no $E=0$ states. There is a rather narrow gap of width $\Delta_0=0.198$ centered at $E=0$. The outer gaps are relatively larger. The upper one extends from $E=[(3-\sqrt{5})/2]^{1/2}=0.618$ to $E=1$, so the width is $\Delta_1=0.382$. These outer gaps are indirect, as before.

The case $N_a=7, N_b=3$ with two-layer edge roughness has no central gap at all. The band dispersion for odd-symmetry states is

$$E=\pm[1+2c^2\pm(1+4c^4)^{1/2}]^{1/2}, \tag{11}$$

so that $E \rightarrow 0$ for the inner pair of odd bands as $k \rightarrow \pm\pi/2$. The overall bandwidth is $w=6.993$. There is an indirect outer gap extending from $E=(3-\sqrt{5})^{1/2}=0.874$ to $E=[(79+\sqrt{97})/64]^{1/2}=1.178$, thus having width $\Delta_1=0.304$. Of course there is also the gap corresponding to it by $E \rightarrow -E$.

As general trends one finds that as the width N_a increases, the gaps become narrower and their number increases. Also, the wave amplitudes at edge sites for states with E near $\pm w/2$ becomes very small, as may be seen also for the perfectly ordered channel. Thus states near the outer band edges become less sensitive to changes in the boundary roughness for two reasons. One is that they have little amplitude at the boundary, and the other is that the spatial variation is such that they sense only slowly varying components of the roughness. The latter point is most clear from the fact that $E \rightarrow \pm\frac{1}{2}w$ requires $k \rightarrow 0$. This is the effective-mass limit.

DOS and Kubo-Greenwood conductance for an ordered model with $(N_a, N_b)=(10,6)$ and (11,9) are shown in Fig. 8. Note that as expected from the above argument the roughness has less influence near the band extrema. A similar trend is somewhat less pronounced for the random cases in Fig. 4. Narrow gaps in Fig. 8, which show up as dips in the conductance, are not completely resolved in the figure. The area under the $E=0$ peak in the normalized DOS in Fig. 8(b) is 6.0%.

As mentioned above, the localized $E=0$ chain states occur also in the quantum percolation problem[29] in which a tight-binding Hamiltonian, with nearest-neighbor matrix entries $+1$ and diagonal entries either 0 or barrier potential β, is constructed on a square or cubic lattice. For such a model, Kirkpatrick and Eggarter[30] found several kinds of localized, molecular states, including the $E=0$ chain states described here. They found that a finite fraction (depending upon the active site concentration) of the total number of eigenstates were of this type. Thus, in their model, there is a δ-function peak at

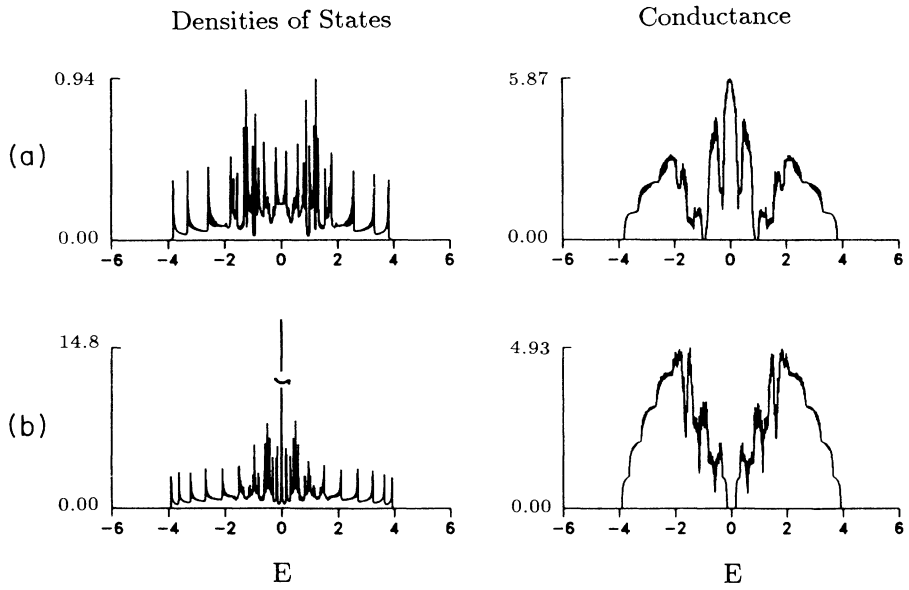

FIG. 8. Densities of states and dc conductance of a Q1D strip with ordered rough edges as depicted in Fig. 1(d) as a function of Fermi energy for two surface roughness conditions. The units of Fermi energy E are the off-diagonal H matrix element. Units of conductance Γ are e^2/h. Energy band for a Q1D ordered rough edge for cases. (a) $N_a=10, N_b=6$, (b) $N_a=11$, $N_b=9$. Note the gaps, some of which appear only as dips in the conductance. The $E=0$ peak in the DOS of (b) represents a finite area and extends orders of magnitude above the rest of the spectrum.

$E=0$ in the average DOS which accounts for a finite area. This is similar to what is found in the current work where the chain states are induced by edge roughness. It has recently been proven[31] that in the quantum percolation model the set of energies of localized molecular states is actually dense in the spectrum. The proof given in Ref. 31 cannot be applied, however, to the rough-channel models when edge roughness is restricted to a few outer rows of atoms.

It is also shown in Ref. 30 that a dip develops in the DOS in the region about $E=0$ which contains the peak due to chain states. The dip indicates a depletion of other states and becomes more pronounced as the concentration of barrier sites increases or as the concentration of active sites decreases below the percolation threshold. The DOS in the dips appears to go smoothly to zero as $E\rightarrow 0$, in the quantum percolation case. Also, as measured by sensitivity to boundary conditions at the edge of a finite sample, states in the central dip near $E=0$ for that model appear to be localized.

In the current work we find for the Q1D ribbons with random rough edges only a slight indication of a decrease in the DOS near the $E=0$ peak. There is, however, a very well defined mobility gap about $E=0$, the width of which increases with increasing disorder or decreasing channel width. Regarding channel width, the mobility gap behaves rather differently depending upon whether the width N_a is odd or even. We suspect that the cause or the nature of the gap (or gaps) in the Q1D models with random rough edges studied here may be slightly different from what is in the percolation case since it may have something to do with residual periodicity. That is, gaps might be induced by Fourier components of the edge roughness.

Conductance results presented thus far apply to Q1D models. The conductance of the Q2D model pictured in Fig. 1(e) with minimal surface roughness ($p=0.02$) and the maximum first- and second-layer roughness are presented in Figs. 9(a) and 9(b), respectively. These have been computed by convolution from Q1D results. The

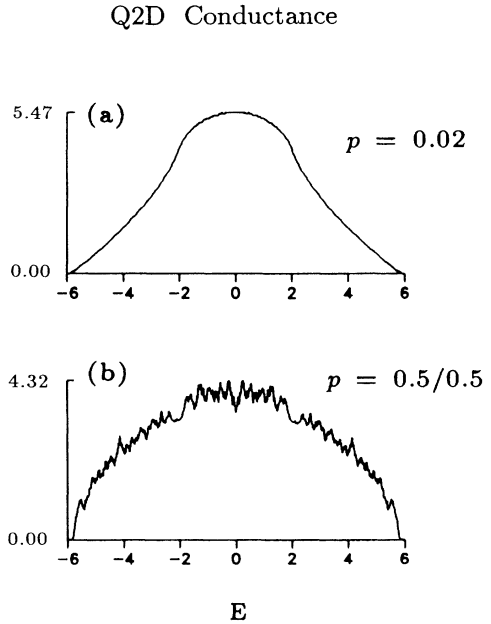

FIG. 9. Conductance for Q2D channels with thickness $N=10$. The units of Fermi energy E are the off-diagonal H matrix element. Units of conductance Γ are e^2/h. (a) Nearly perfectly ordered case ($p=0.02$). (b) Maximum random roughness at the outer layers.

conductance is obtained using Q1D conductance for Γ_1 and the analytical 1D DOS for D_1 in Eq. (2). The effects of such washboard roughness in the Q2D model on either the DOS or the conductance are not dramatic. Much of the structure has washed out in convolution.

There are also localized states in the Q2D channel with wave functions having diagonal chainlike variation in Q1D and traveling-wave-like behavior in the z direction. Thus they carry no current along the channel. These have energies distributed continuously between -2 and $+2$ and account for a decrease in conductance within this energy range. If a fully 2D surface roughness were included, rather than washboard roughness, which is translation symmetric along the z axis, then other kinds of localized states would appear. For example, there would again be a peak in the Q2D DOS at $E=0$ caused by states with nonzero amplitudes of alternating ± 1 in a line along a cubic diagonal. It might be expected that, in analogy with the case of quantum percolation, there would also be a depletion of other states in the energy range near $E=0$. The conductance would again be expected to have a gap about $E=0$, as in the Q1D case.

In summary, we have presented a study of surface roughness on transport in narrow tight-binding channels. As a starting point, Eqs. (1)–(8) give results for perfectly ordered cases against which one can compare. These formulas follow from Eq. (1), which expresses conductance across a section of a perfect 1D chain, which is in turn attached to perfect leads, in the limit $\eta \rightarrow 0$. It is possible to retain a finite η.[32] The result of doing so is to introduce a small, constant optical potential which makes eigenstates decay slowly in time. While one might imagine this represents some realistic inelastic effect, it is completely *ad hoc*.

We believe that Eq. (6), which is the $N \rightarrow \infty$ limit of Eq. (4) divided by the width N, has not been published before. The order of limits it represents is first $L \rightarrow \infty$, then $\eta \rightarrow 0$, and finally $N \rightarrow \infty$. The sheet conductance diverges in such a way that the shape function in Eq. (6), which has been appropriately rescaled, remains finite. The ordered channel results are thus obtained naturally from the extension formulas.

The results for models with edge roughness show that the effects are weak near the band extrema where the DOS and conductance do not vary remarkably from the perfect channel case. This is the effective-mass limit in which the theory of Ref. 1 applies well.

On the other hand, spectral features near the middle of the band are strongly disrupted with the appearance of gaps and, at least at $E=0$, of highly localized states. These features are adequately well understood. There is a surprising correlation between the cases of random and periodic edge roughness.

One must note that the interesting features in the middle of the band occur where the intrinsic granularity becomes important and where the continuum wave interpretation breaks down. Also, these features, particularly the $E=0$ peak, are not robust with respect to small changes in the model. For example, we have seen that the existence of the $E=0$ states in the ordered rough edge case depends on the relation $N_b=N_a-2$ with N_a odd. Random models are more robust, but the characteristics of the midband spectral or conductance features would be quite different on a triangular lattice or in the case of a realistic tight-binding model. One would not therefore be able to apply the current results directly to an actual thin channel. What is learned, however, is that roughness can cause relatively dramatic changes in conductance in the center of the band including the introduction of gaps and strongly localized states.

To apply the predictions to experimental results at all, it would be necessary to look at cases with good transverse confinement. The characteristic length scale for roughness should also be relatively small. In the Q1D case it would seem that these conditions are best met in quantum wires fabricated either by a substrate step technique[33] or else by molecular-beam epitaxy onto a surface misoriented by a few degrees from a main crystallographic direction.[34] It would not be reasonable to compare the current models to cases where the conducting channel is constrained laterally by a depletion region, as in split-gate wires, where potential fluctuations resulting from charge accumulation occur on a longer length scale.[35] Similarly, in the Q2D case, the calculations would seem most applicable to narrow quantum wells deposited by molecular-beam epitaxy or to ultrathin crystal layers.[36]

The authors acknowledge a helpful correspondence with Philip Bagwell, who brought Ref. 27 to our attention. We thank J. Davies for pointing out the work of Kirkpatrick and Eggarter (Ref. 30) and of Chayes *et al.* (Ref. 31) on localized states in quantum percolation. One of us (W.A.S.) is grateful to Song He for a discussion concerning implementation of the conductance formula of Ref. 5. We are also grateful for communications between the other author (M.K.S.) and Roger Haydock who pointed out the nature of the $E=0$ states in the random models. Computer time was provided by Cornell National Supercomputer Facility. The work was partially funded by National Science Foundation Grant No. DMR-8705879.

*On leave from Physics Department, University of North Dakota, Grand Forks, ND 58202-8008.

[1]Z. Tešanović, M. V. Jarić, and S. Maekawa, Phys. Rev. Lett. **57**, 2760 (1986).

[2]Z. Tešanović, J. Phys. C **20**, L829 (1987).

[3]J. Phillips *et al.*, Appl. Phys. Lett. **51**, 1895 (1987).

[4]P. A Badoz *et al.*, Appl. Phys. Lett. **51**, 169 (1987).

[5]P. A. Lee and T. V. Ramakrishnan, Rev. Mod. Phys. **57**, 287 (1985); A. H. Nayfeh, *Perturbation Methods* (Wiley, New York, 1973), Sec. 7.4.1.

[6]Song He and S. Das Sarma, Phys. Rev. B **40**, 3379 (1989).

[7]F. Sols, M. Macucci, U. Ravaioli, and K. Hess, Appl. Phys. Lett. **54**, 350; J. Appl. Phys. **66**, 3892 (1989).

[8]E. G. Haanappel and D. van der Marel, Phys. Rev. B **39**, 5484

(1989); D. van der Marel and E. G. Haanappel, *ibid.* **39**, 7811 (1989).
[9]P. A. Lee and D. S. Fisher, Phys. Rev. Lett. **47**, 882 (1981).
[10]W. A. Schwalm and M. K. Schwalm, Phys. Rev. B **37**, 9524 (1988).
[11]P. F. Bagwell and T. P. Orlando, Phys. Rev. B **40**, 1456 (1989).
[12]R. Landauer, Philos. Mag. **21**, 863 (1970); M. Büttiker, Y. Imry, R. Landauer, and S. Pinhas, Phys. Rev. B **31**, 6207 (1985).
[13]E. N. Economou and C. M. Soukoulis, Phys. Rev. Lett. **46**, 618 (1981).
[14]D. S. Fisher and P. A. Lee, Phys. Rev. B **23**, 6851 (1981).
[15]H. U. Baranger and A. D. Stone, Phys. Rev. B **40**, 8169 (1989).
[16]C. Coulson, Proc. Cambridge Philos. Soc. **36**, 193 (1940).
[17]B. J. van Wees *et al.*, Phys. Rev. Lett. **60**, 848 (1988); Phys. Rev. B **38**, 3625 (1988).
[18]D. A. Wharam *et al.*, J. Phys. C **21**, L209 (1988).
[19]G. Kirczenow, Solid State Commun. **68**, 715, (1988); Phys. Rev. B **39**, 10 452 (1989).
[20]L. I. Glazman and A. V. Khaetskii, Pis'ma Zh. Eksp. Teor. Fiz. **48**, 546 (1988) [JETP Lett. **48**, 591 (1988)]; L. I. Glazman, G. B. Lesovik, D. E. Khmelńitskii and R. I. Shekhter, *ibid.* **48**, 218 (1988) [*ibid.* **48**, 238 (1988)].
[21]E. Castaño and G. Kirczenow, Solid State Commun. **70**, 801 (1989); Phys. Rev. B **41**, 5055 (1990).
[22]A. Kawabata, J. Phys. Soc. Jpn. **58**, 372 (1989).
[23]A. Szafer and A. D. Stone, Phys. Rev. Lett. **62**, 300 (1989).
[24]Y. Avishai, M. Kaveh, S. Shatz, and Y. B. Band, J. Phys. Condens. Matter **1**, 6907 (1989).
[25]A. Yacoby and Y. Imry, Phys. Rev. B **41**, 5341 (1990).
[26]M. Büttiker, Phys. Rev. B **41**, 7906 (1990).
[27]P. F. Bagwell, Phys. Rev. B **41**, 10 354 (1990).
[28]P. Anderson, Phys. Rev. **109**, 1492 (1958).
[29]P. de Gennes, P. Lafore, and J. Millot, J. Phys. Chem. Solids **11**, 105 (1959).
[30]S. Kirkpatrick and T. P. Eggarter, Phys. Rev. **6**, 3598 (1972).
[31]J. T. Chayes, L. Chayes, J. Franz, J. Sethna, and S. Trugman, J. Phys. A **19**, L1173 (1986).
[32]D. J. Thouless and S. Kirkpatrick, J. Phys. C **14**, 235 (1981).
[33]D. Prober, M. Feuer, and N. Giodano, Appl. Phys. Lett. **37**, 94 (1980).
[34]P. Petroff, A. Gossard, and W. Wiegmann, Appl. Phys. Lett. **45**, 620 (1984).
[35]J. Nixon and J. Davies, Phys. Rev. B **41**, 7929 (1990).
[36]H. Soonpaa and W. Schwalm, Phys. Lett. **100A**, 156 (1984).